DOI: 10.6060/mhc245823o

meso-Bromination Greatly Enhances Reactivity of Cyanocobalamin towards Hydrogen Sulfide

Vladimir S. Osokin, Ilia A. Dereven'kov, Anna S. Makarova, Pavel A. Molodtsov, and Sergei V. Makarov[@]

Ivanovo State University of Chemistry and Technology, 153000 Ivanovo, Russia
[@]Corresponding author E-mail: makarov@isuct.ru

Here, we showed that in contrast to the unmodified complex cyanocobalamin brominated at the C10 position of the macrocycle (CNCbl-Br) can be reduced by hydrogen sulfide to the Co(II) complex (Cbl(II)-Br). Unlike glutathione, hydrogen sulfide is capable of attacking the C-Br bond in Cbl(II)-Br, resulting in debromination of the macrocycle. A reaction mechanism including a slow 5,6-dimethylbenzimidazole dissociation step, subsequent rapid binding of hydrogen sulfide to the Co(III) ion, and electron transfer from the sulfur atom to the Co(III)-ion was suggested. Due to the high reactivity of brominated cobalamin towards hydrogen sulfide, it can be recommended for further study as a potential antidote for this toxin.

Keywords: Cyanocobalamin, bromination, hydrogen sulfide, kinetics, mechanism.

мезо-Бромирование – эффективный способ повышения скорости реакции цианокобаламина с сероводородом

В. С. Осокин, И. А. Деревеньков, А. С. Макарова, П. А. Молодцов, С. В. Макаров

Ивановский государственный химико-технологический университет, 153000 Иваново, Россия
[@]E-mail: makarov@isuct.ru

Показано, что, в отличие от немодифицированного цианокобаламина, бромированный в положении C10 макроцикла цианокобаламин (CNCbl-Br) восстанавливается сероводородом до Co(II) комплекса (Cbl(II)-Br). В отличие от глутатиона, сероводород способен атаковать связь C-Br в Cbl(II)-Br, что приводит к дебромированию макроцикла. Предложен механизм реакции, включающий медленную стадию отщепления 5,6-диметилбензимидазола, последующее быстрое присоединение сероводорода к иону Co(III) и перенос электрона от атома серы к иону Co(III). Высокая реакционная способность бромированного цианокобаламина по отношению к H_2S открывает перспективы использования этого комплекса в качестве антидота для сероводорода.

Ключевые слова: Цианокобаламин, бромирование, сероводород, кинетика, механизм.

Introduction

Among vitamins, vitamin B_{12} (cobalamin; Cbl) attracts special attention due to its complex structure and interesting (bio)chemistry.[1] A large number of works reports cobalamin structural alterations that allow to produce complexes with desired properties. In particular, introduction the aryl motifs into the upper axial position of Cbl produces species with antivitamin characteristics.[2] Cobalamins (Cbls) can participate in reactions of 5,6-dimethylbenzimidazole nucleotide

(DMBI) elimination to form cobinamide,[3,4] formation of lactam and lactone rings,[5,6] *meso*-modification,[7] with the greatest attention paid to the reactions of introducing halogens into the C10 position of the macrocycle.[8–11]

The introduction of halogen atoms into the C10-position of cyano- (CNCbl) and aqua- (H_2OCbl) cobalamins greatly affects their chemical properties. In particular, brominated CNCbl (CNCbl-Br) (Figure 1) can be reduced by glutathione to the Co(II) form in a neutral medium, whereas the reaction involving unmodified CNCbl does not occur.[10] This feature represents interest for the preparation of cobalamins possessing vitamin properties for patients with genetic disorders of vitamin B_{12} metabolism.[12,13] In contrast to unmodified CNCbl, *meso*-chlorinated CNCbl and CNCbl-Br react with nitroxyl (HNO) to give nitrosyl complexes exhibiting higher aerobic stability than unmodified nitrosylcobalamin.[14] Some *meso*-brominated cobalamins act as antimetabolites that was shown using *Lactobacillus delbrueckii*.[15,16] Carbon monoxide donors based on *meso*-chlorinated and brominated cobalamins have been obtained.[9]

H_2OCbl and aquahydroxocobinamide are highly reactive towards hydrogen sulfide.[17,18] Although aquahydroxocobinamide significantly reduces toxic effects caused by H_2S,[19,20] H_2OCbl is less efficient as antidote.[21] *meso*-Modification can increase the reactivity of cobalamins towards H_2S and improve their antidote performance against this toxin. In this work, we evaluated the influence of *meso*-bromination on the reactivity of CNCbl towards H_2S.

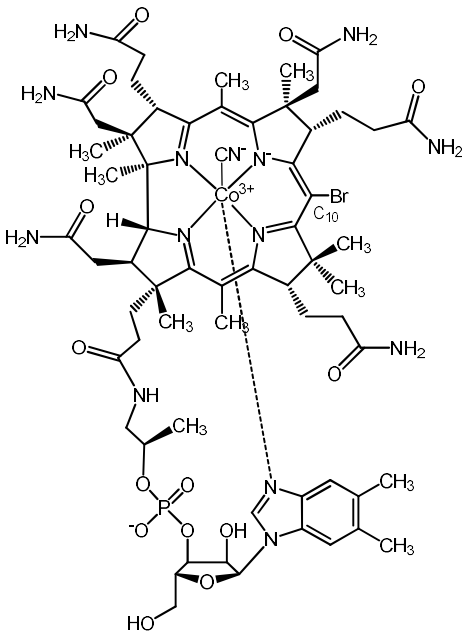

Figure 1. Structure of *meso*-brominated cyanocobalamin.

Experimental

Cyanocobalamin (Sigma-Aldrich; ≥ 98%), tris(2-carboxyethyl)phosphine hydrochloride (TCEP; Sigma-Aldrich), N-bromosuccinimide (Alfa Aesar; 99%) and trifluoroacetic acid (Sigma-Aldrich; 99%) were used without additional purification. Other chemicals were of analytical reagent grade. Oxygen-free argon was used to deoxygenate reagent solutions. Buffer solutions (phosphate, borate and carbonate; 0.1 M) were used to maintain the p*H* during the measurements. Hydrogen sulfide solution was prepared via saturation of deoxygenated water by H_2S generated via dropwise adding concentrated orthophosphoric acid to dry sodium sulfide nonahydrate. H_2S concentrations were determined spectrophotometrically[22]. TCEP sulfide was prepared via mixing stoichiometric quantities of TCEP dissolved in water and S_8 under anaerobic conditions. CNCbl-Br was synthesized from CNCbl via the reported procedure,[9] *i.e.*, small portions of solid N-bromosuccinimide were slowly added to CNCbl solution in glacial acetic acid. Primary purification was performed using column chromatography on silica gel (Macherey-Nagel Silica 60, 0.04–0.063 mm). The column was washed with water and the crude product was eluted by 20% (v/v) aqueous ethanol. Fine purification was carried out using semi-preparative HPLC. The following gradient was employed: 5% acetonitrile / 95% (water + 0.03% trifluoroacetic acid) (0 min) to 40% acetonitrile / 60% (water + 0.03% trifluoroacetic acid) (20 min). The fraction with R_t = 14.2 min was collected, which corresponds to CNCbl-Br. UV-Vis λ_{max} nm: 365, 549, 576. MALDI MS *m/z* (positive ion mode): 1408.7 (Cbl-^{79}Br + H), 1410.7 (Cbl-^{81}Br + H).

UV-Vis spectra were recorded with a thermostated (±0.1 °C) Shimadzu UV-1800 spectrophotometer in quartz cells under anaerobic conditions. CNCbl-Br was purified on a Stayer M (Akvilon, Russia) system equipped with a Cosmosil (5C18-MS-II) C18ec RP column (5 μm particle size; 250×10 mm; flow rate is 3 mL/min). MALDI-MS measurements were performed on a Shimadzu AXIMA Confidence mass-spectrometer with 2,5-dihydroxybenzoic acid as the matrix.

Experimental data were analyzed using OriginPro 2018 software.

Results and Discussion

Mixing H_2S with CNCbl-Br solution results in the changes in the UV-Vis spectrum indicated in Figure 2A: a decrease in the absorption maxima of Br-CNCbl at 576 and 365 nm is observed, as well as an increase in absorbance at 370–500 and above 590 nm due to the formation of elemental sulfur in the course of the reaction. It, in turn, most likely absorbs Br-CNCbl; this explains the disappearance of all its absorption bands. To prevent the precipitation of sulfur interfering with the reaction control, TCEP was introduced into the solution prior to adding H_2S, which binds sulfur at a high rate to form phosphine sulphide.[23] Preliminary experiments showed that TCEP does not react with CNCbl-Br (Figure S1). UV-Vis spectra collected for the reaction between CNCbl-Br and H_2S in the presence of TCEP are shown in Figure 2B: an increase in absorbance at 474–494 nm is observed, and the UV-vis spectrum of the product corresponds to the Cbl(II)-Br.[10] The reaction between H_2S and unmodified CNCbl does not proceed (Figure S2).

Incubation of H_2S with CNCbl-Br for 24 h is accompanied by the further changes in UV-Vis spectrum (Figure S3): the absorption maximum shifts from 485 to 475 nm. The UV-Vis spectrum of the reaction product coincides with that of unmodified Cbl(II). Adding the excess of potassium cyanide to the final product of the reaction of H_2S with CNCbl-Br under aerobic conditions leads to the formation of a complex with absorption maxima at 360, 519 and 551 nm (Figure S3), which corresponds to unmodified CNCbl. The MALDI mass-spectrum of the product formed during prolonged incubation of a mixture H_2S–CNCbl-Br and subsequent addition of an aerobic cyanide solution is shown in Figure S4A: the signal of the molecular ion is shifted relative to the signal of CNCbl-Br (Figure S4B) by 79 units and coincides with the signal of unmodified CNCbl

(Figure S4C). Prolonged incubation of the mixture of CNCbl-Br with glutathione (GSH) does not lead to debromination of the macrocycle.

The kinetics of the reaction between CNCbl-Br and H_2S was studied in the presence of TCEP. A typical reaction kinetic curve obtained using a tenfold excess of H_2S over CNCbl-Br is shown in Figure 3A. Its profile is characteristic of an autocatalytic process. To determine the reason of acceleration of the reaction between CNCbl-Br and hydrogen sulfide in the presence of TCEP, the effect of TCEP sulfide on the stability of CNCbl-Br was assessed. We found that TCEP sulfide reduces CNCbl-Br to Cbl(II)-Br (Figure S5A), and the kinetic curve of the reaction is linear (Figure S5B). The slope of the kinetic curves for the reaction of CNCbl-Br with TCEP sulfide does not depend on CNCbl-Br concentration (Figure S5B), indicating a zero-order reaction with respect to CNCbl-Br. Thus, CNCbl-Br is not involved in the rate-determining step during reduction in the presence of phosphine sulfide. The rate-limiting stage of this process is not clearly understood: it is likely that TCEP sulfide is slowly destroyed to form a highly reactive sulfur species, which reduces CNCbl-Br to Cbl(II)-Br at a high rate. We found that in the presence of TCEP sulfide, the conversion of CNCbl to Cbl(II) does not occur (Figure S6).

To study the kinetics of the reaction of CNCbl-Br with H_2S (*i.e.* without TCEP), the initial slopes of the kinetic curves were used, where the influence of phosphine sulfide is negligible. The observed rate constants ($k_{obs.}$) were obtained by dividing the initial reaction rates by the initial concentration of CNCbl-Br. Linear dependence $k_{obs.}$ on [H_2S] (Figure 3B) proves the first order with respect to H_2S, it exhibits a positive Y-intercept, which origin can be explained by the existence of the reverse reaction.

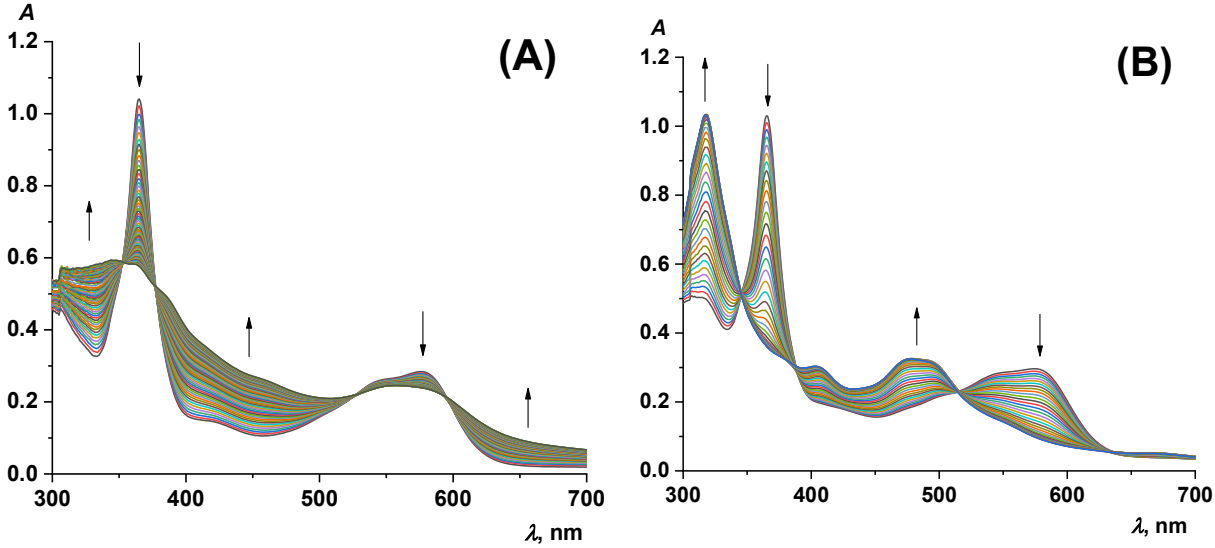

Figure 2. UV-Vis spectra recorded for the reaction between CNCbl-Br ($3.1 \cdot 10^{-5}$ M) and H_2S ($5.0 \cdot 10^{-3}$ M) in the absence (A) and presence (B) of TCEP ($1.0 \cdot 10^{-3}$ M) at p*H* 7.4, 25.0 °C. Spectra were recorded for 70 min, time interval between spectra is 60 s.

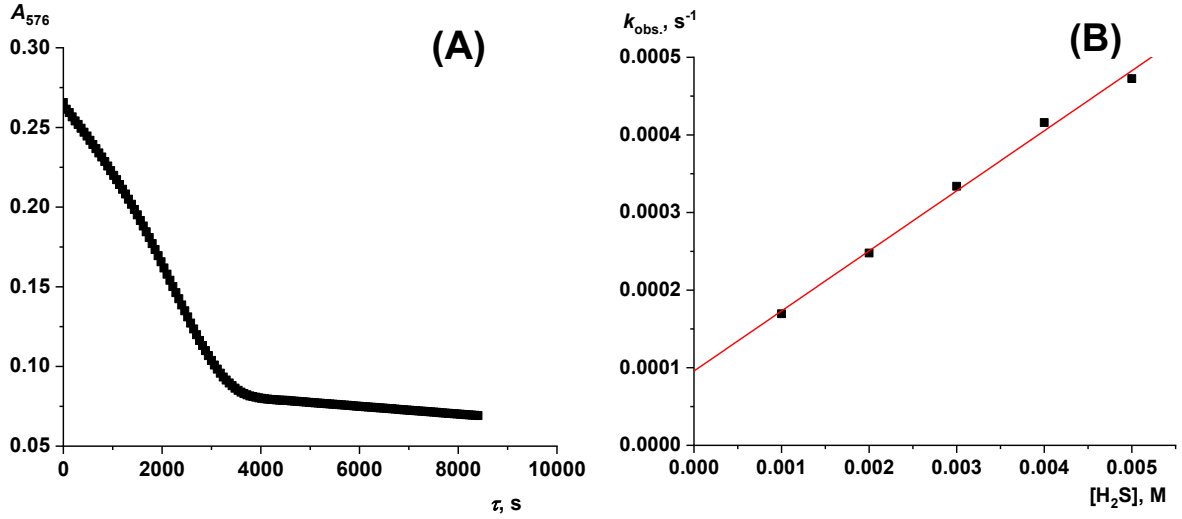

Figure 3. (A) Kinetic curve of the reaction between CNCbl-Br ($3.1 \cdot 10^{-5}$ M) and H_2S ($5.0 \cdot 10^{-3}$ M) in the presence of TCEP ($1.0 \cdot 10^{-3}$ M) at p*H* 7.4, 25.0 °C. (B) Dependence of observed rate constant ($k_{obs.}$) of the reaction between CNCbl-Br ($3.1 \cdot 10^{-5}$ M) and H_2S in the presence of TCEP ($1.0 \cdot 10^{-3}$ M) on [H_2S] at p*H* 7.4, 25.0 °C

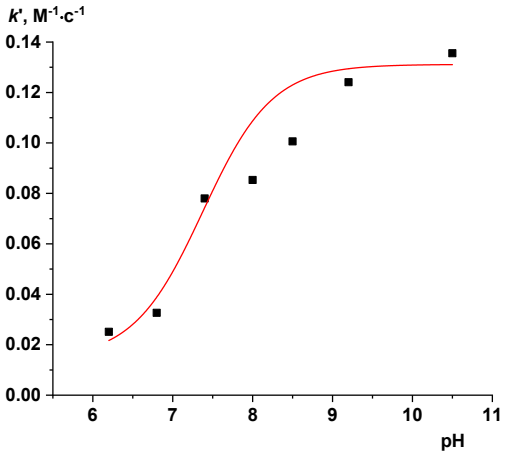

Figure 4. Plot of *k*' versus p*H* at 25 °C (points) and its fitting to Eq. (2; line).

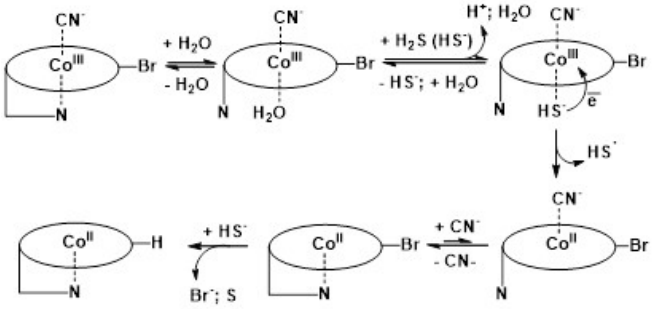

Scheme 1. Mechanism of the reaction between CNCbl-Br and H_2S.

We found that the slope of the dependence of k_{obs} on [H_2S] (*k*') increases with decreasing acidity of the medium (Figure 4): the plot of *k*' versus p*H* has the shape of a sigmoid curve with an inflection point at *ca*. p*H* 7.5. Acid-base properties of CNCbl-Br remain unchanged in this range,[10] whereas hydrogen sulfide exists also in the deprotonated form in neutral medium (pK_a = 7.0;[22] reaction 1). Thus, the acceleration of the reaction with increasing p*H* can be explained by the formation of hydrosulfide in the solution, which possesses stronger nucleophilic properties.

$$H_2S \leftrightarrow H^+ + HS \qquad (1;\ pK_a).$$

Assuming the reduction of CNCbl-Br with hydrosulfide and hydrogen sulfide, equation (2) was derived.

$$k' = k_1 \frac{10^{pK_a}}{10^{pH} + 10^{pK_a}} + k_2 \frac{10^{pH}}{10^{pH} + 10^{pK_a}} \qquad (2)$$

where k_1 and k_2 are rate constants for the reaction of Br-CNCbl with H_2S and HS^- ($M^{-1}\cdot s^{-1}$), respectively. Fitting the plot presented in Figure 4 to Eq. (2) gives $k_1=(1.4 \pm 0.8)\cdot 10^{-2}$ $M^{-1}\cdot s^{-1}$ and $k_2 = (0.13 \pm 0.01)$ $M^{-1}\cdot s^{-1}$.

In our previous work, we showed that the reaction between CNCbl-Br and GSH proceeds via a rate-determining DMBI dissociation step, successive GSH binding, and electron transfer from the sulfur atom to the Co(III)-ion.[10] Here we assume the similar tentative mechanism. The first step of the reaction between CNCbl-Br and H_2S is the slow DMBI dissociation as well (Scheme 1) followed by rapid binding of H_2S/HS^-. The reaction involving the dissociation of cyanide is unlikely due to the very high value of CN^- binding constant with Cbl(III).[24] Cbl(II)-Br is formed during subsequent electron transfer from hydrogen sulfide to Co(III)-ion, which produces sulfanyl radical as well. The successive stages result in the formation of elemental sulfur. Nucleophilic attack of HS^- to the C-Br bond in Cbl(II)-Br and CNCbl-Br leads to dehalogenation of the complex.

Conclusions

The work shows that *meso*-bromination makes possible the reduction of CNCbl with hydrogen sulfide, which is associated with the weakening of the Co(III)-DMBI bond in CNCbl-Br as compared to CNCbl. In contrast to the reaction of CNCbl-Br with glutathione, the reaction with H_2S leads not only to the formation of Cbl(II)-Br, but also to dehalogenation of the macrocycle. We suggest a reaction mechanism including a rate-determining DMBI dissociation, subsequent rapid binding of hydrogen sulfide to the Co(III)-ion and electron transfer from the sulfur atom to the Co(III)-ion. Further research may be aimed at studying the reactions of hydrogen sulfide with halogenated forms of aquacobalamin. Due to the high reactivity of brominated cobalamin towards hydrogen sulfide, it can be recommended for further study as a potential antidote for this toxin.

References

1. Erina A.A., Borodulin V.B., Dereven'kov I.A., Makarov S.V., Ischenko A.A. *ChemChemTech [Izv. Vyssh. Uchebn. Zaved. Khim. Khim. Tekhnol.]* **2024**, *67*(7), 6–18.
2. Ruetz M., Gherasim C., Gruber K., Fedosov S., Banerjee R., Kräutler B. *Angew. Chemie Int. Ed.* **2013**, *52*, 2606–2610.
3. Zhou K., Zelder F. *J. Porphyrins Phthalocyanines* **2011**, *15*, 555–559.
4. Dereven'kov I.A., Salnikov D.S., Shpagilev N.I., Makarov S.V., Tarakanova E.N. *Macroheterocycles* **2012**, *5*, 260–265.
5. Chemaly S.M., Brown K.L., Fernandes M.A., Munro O.Q., Grimmer C., Marques H.M. *Inorg. Chem.* **2011**, *50*, 8700–8718.
6. Pugina R.A., Denisova E.A., Ivlev P.A., Salnikov D.S., Makarov S.V. *J. Porphyrins Phthalocyanines* **2018**, *22*, 1092–1098.
7. Wierzba A.J., Wincenciuk A., Karczewski M., Vullev V.I., Gryko D. *Chem. Eur. J.* **2018**, *24*, 10344–10356.
8. Ghadimi N., Perry C.B., Fernandes M.A., Govender P.P., Marques H.M. *Inorg. Chim. Acta* **2015**, *436*, 29–38.
9. Prieto L., Rossier J., Derszniak K., Dybas J., Oetterli R.M., Kottelat E., Chlopicki S., Zelder F., Zobi F. *Chem. Commun.* **2017**, *53*, 6840–6843.
10. Dereven'kov I.A., Osokin V.S., Khodov I.A., Sobornova V.V., Ershov N.A., Makarov S.V. *JBIC J. Biol. Inorg. Chem.* **2023**, *28*, 571–581.
11. Dereven'kov I.A., Osokin V.S., Hannibal L., Makarov S.V., Khodov I.A., Koifman O.I. *JBIC J. Biol. Inorg. Chem.* **2021**, *26*, 427–434.
12. Esser A.J., Mukherjee S., Dereven'kov I.A., Makarov S.V., Jacobsen D.W., Spiekerkoetter U., Hannibal L. *iScience* **2022**, *25*, 104981.

13. Wingert V., Mukherjee S., Esser A.J., Behringer S., Tanimowo S., Klenzendorf M., Derevenkov I.A., Makarov S.V., Jacobsen D.W., Spiekerkoetter U., Hannibal L. *Biochimie* **2021**, *183*, 108–125.
14. Dereven'kov I.A., Osokin V.S., Ershov N.A., Makarov S.V. *J. Porphyrins Phthalocyanines* **2024**, *28*, 217–224.
15. Mestizo P.D., Brenig C., Stephan R., Zelder F., Muchaamba F. *LWT* **2024**, *191*, 115641.
16. Brenig C., Mestizo P.D., Zelder F. *RSC Adv.* **2022**, *12*, 28553–28559.
17. Salnikov D.S., Kucherenko P.N., Dereven'kov I.A., Makarov S.V., van Eldik R. *Eur J. Inorg. Chem.* **2014**, *5*, 852–862.
18. Salnikov D.S., Makarov S.V., van Eldik R., Kucherenko P.N., Boss G.R. *Eur. J. Inorg. Chem.* **2014**, *2014*, 4123–4133.
19. Hendry-Hofer T.B., Ng P.C., McGrath A.M., Mukai D., Brenner M., Mahon S., Maddry J.K., Boss G.R., Bebarta V.S. *Ann. N Y Acad. Sci.* **2020**, *1479*, 159–167.
20. Brenner M., Benavides S., Mahon S.B., Lee J., Yoon D., Mukai D., Viseroi M., Chan A., Jiang J., Narula N., Azer S.M., Alexander C., Boss G.R. *Clin. Toxicol.* **2014**, *52*, 490–497.
21. Bebarta V.S., Garrett N., Brenner M., Mahon S.B., Maddry J.K., Boudreau S., Castaneda M., Boss G.R. *Acad. Emerg. Med.* **2017**, *24*, 1088–1098.
22. Hughes M.N., Centelles M.N., Moore K.P. *Free Radic. Biol. Med.* **2009**, *47*, 1346–1353.
23. Bartlett P.D., Meguerian G. *J. Am. Chem. Soc.* **1956**, *78*, 3710–3715.
24. George P., Irvine D.H., Glauser S.C. *Ann. N Y Acad. Sci.* **1960**, *88*, 393–415.

Received 07.04.2024
Accepted 06.12.2024